Microcavity-like leaky mode emission from a planar optical waveguide made of luminescent silicon nanocrystals

J. Valenta[a] and T. Ostatnický
Department of Chemical Physics & Optics, Faculty of Mathematics & Physics, Charles University, Ke Karlovu 3, CZ-121 16 Prague 2, Czech Republic

I. Pelant
Institute of Physics, Academy of Sciences of the Czech Republic, Cukrovarnicka 10, CZ-162 53 Prague 6, Czech Republic

R. G. Elliman
Electronic Materials Engineering Department, Research School of Physical Sciences and Engineering, Australian National University, Canberra ACT 0200, Australia

J. Linnros
Department of Microelectronics & Information Technology, Royal Institute of Technology, Electrum 229, S-164 40 Kista-Stockholm, Sweden

B. Hönerlage
IPCMS, Groupe d'Optique Nonlinéaire et d'Optoéléctronique, UMR 7504 CNRS-ULP, 23, rue du Loess, 67037 Strasbourg Cedex, France

(Received 3 May 2004; accepted 2 August 2004)

The propagation of light emitted from silicon nanocrystals forming planar waveguides buried in SiO_2 is studied both experimentally and theoretically. Experiments reveal that photoluminescence spectra detected from the sample facet mainly contains narrow (10–20 nm full-with-at-half-maximum) polarization-resolved transverse electric and transverse magnetic modes instead of the usual broad nanocrystal emission band peaked at 700–800 nm. A theoretical model developed in the framework of wave optics identifies these modes as substrate modes propagating along the waveguide boundary (*not* the usual modes guided inside the nanocrystal plane due to its graded index profile). This peculiar observation is the consequence of the high losses in the nanocrystalline waveguide and may occur in other dissipative waveguide structures under conditions that are discussed. © *2004 American Institute of Physics*. [DOI: 10.1063/1.1795984]

I. INTRODUCTION

Light-emitting silicon nanostructures have attracted considerable interest since the discovery of bright visible photoluminescence (PL) in porous silicon by Canham.[1] This interest has been further stimulated by recent reports of optical gain in an ensemble of silicon nanocrystals (Si-NCs).[2–7] Most of the investigators looking for optical gain use samples in the form of a thin Si-NC layer (prepared either by the Si-ion implantation or by the plasma-enhanced chemical vapour deposition method) embedded in a transparent silica matrix, or Si/SiO_2 superlattices. Such structures work as asymmetric *active* planar optical waveguides, where the light is not coupled to the core from outside but originates from an ensemble of emitting Si-NCs inside the waveguide.

Here we report on experimental observations of unusual PL from planar waveguides made of luminescent Si-NCs in SiO_2 matrix. In particular, a significant narrowing of PL lineshape and splitting of the emission into spectrally separated transverse electric (TE) and transverse magnetic (TM) modes. Such behavior is very similar to III-V semiconductor-based microcavity PL TE-TM splitting observed in directions different from surface normal.[8,9] We show that the narrow TE and TM modes, which the waveguide self-selects from a wide spontaneous emission spectrum, are not the usual guided modes, as assumed in our earlier report, but leaky substrate modes. They arise from constructive Fabry-Perot interference of luminescence rays leaving the active Si-NC layer to the substrate near the angle of total internal reflection. The existence of such modes is a general property of thin luminescent layers, irrespective of whether they are in the form of semiconductor microcavities.[9,10] or simple organic/inorganic thin films.[11,12] Hereafter, we deal with a general case of an asymmetric planar waveguide with a graded index profile where these modes are extremely well developed. We show, both experimentally and theoretically, that such experimental dominance of the leaky modes depends strongly upon a coincidence of several parameters, including the waveguide losses experienced by guided modes, the refractive index contrast of the core and cladding and the depth of core layer within the substrate.

II. SAMPLE PREPARATION AND EXPERIMENTAL SET-UPS

The samples used in this study were prepared by implanting 400 keV Si^+ ions into 1 nm thick silica slab (Infrasil) with optically polished surface and edges. Implantation

[a]Author to whom correspondence should be addressed; electronic mail: jan.valenta@mff.cuni.cz

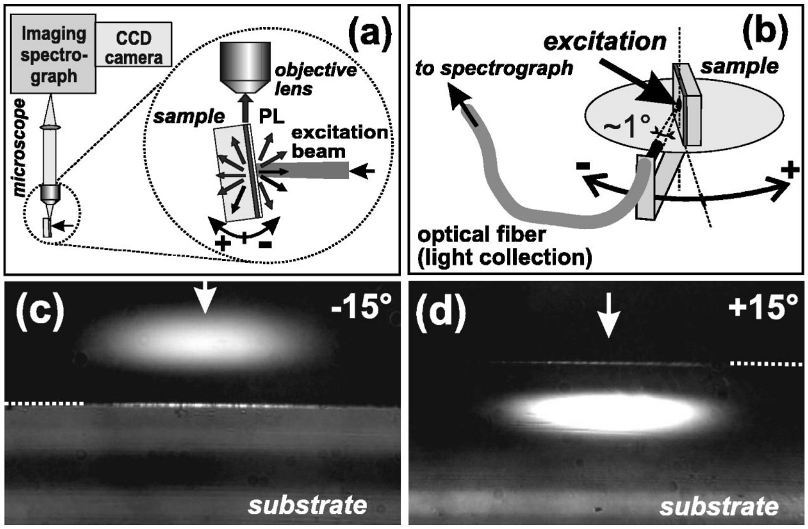

FIG. 1. Sketch of the experimental geometry for the microPL setup (a) and for the goniometer setup (b). Lower panels show PL intensity images (area 2×1.2 mm^2) of the excited waveguide (using micro-PL setup) for sample inclination of $\alpha = -15°$ (c) and $\alpha = +15°$ (d). The elliptical spot is the excited region on the surface of the sample, and the narrow line is the PL emanating from the sample facet. The substrate is slightly illuminated with a white lamp giving rise to the lighter gray color in the bottom part of the images. The white arrows indicate the direction of excited beam.

doses of 3, 4, 5, and 6×10^{17} Si cm^{-2} (in four different regions of the slab) were chosen to produce different levels of refractive index contrast between the core and cladding/substrate layers. Peak excess Si concentrations were up to 26 at. % Si. Implanted samples were subsequently annealed for 1 h in N_2 ambient at 1100 °C and 1 h in forming-gas (5% H_2 in N_2) at 500 °C. The presence of Si-NCs in the annealed layers, with diameter between 4–5 nm, was confirmed by Raman scattering (not shown here).

The PL properties of samples were investigated using a continuous wave He-Cd laser (325 nm) as the excitation source (excitation intensity ~0.3 W/cm^2) and a microscope connected to an imaging spectrograph with a CCD camera for detection [Fig. 1(a)]. The detection numerical aperture (NA) was 0.075 (i.e., an angular resolution of about 8.6°). All measurements were performed at room temperature and all PL spectra were corrected for the system response. To achieve better angular resolution a second experimental arrangement was also employed in which the sample was fixed to the centre of a goniometer [Fig. 1(b)]. The PL emission was then collected by a silica optical fiber (core diameter 1 mm) rotated around the sample at a distance of 50 mm, giving an angular resolution slightly less than 1° (NA ~0.01). The output of the fibre was measured using the same detection system described above.

Typical images observed with the microscopic setup [Fig. 1(a)] are illustrated in Figs. 1(c) and 1(d). Here the diameter of the excitation spot, located at about 1 mm from the sample edge, is roughly 1 mm. One can easily recognize PL emission from the excited spot as a bright ellipsoid. However, there is also a second contribution emanating from the facet of the sample. This light is obviously guided in the implanted layer or close to it. The images in Figs. 1(c) and 1(d) were collected for sample inclination angles of −15° and +15°, respectively, i.e., in a geometry for which the excited spot was observed either directly [Fig. 1(c)] or through the substrate [Fig. 1(d)]. The experimental arrangement shown in Fig. 1(a) enables the detection of the PL either from the excited spot or from the edge of sample by positioning the entrance slit of the spectrograph to different locations of the PL image.

III. EXPERIMENTAL RESULTS AND DISCUSSION

Figure 2 (left column) presents PL spectra of four layers produced by implanting to different doses. The broad dotted curves correspond to PL emanating from the sample surface (perpendicularly to the Si-NC layer, i.e., conventional geometry) while the other curves represent PL collected from the facet of the sample (sample inclination was +2.5°). It can be seen that these two types of spectra differ considerably. The facet PL spectra are much narrower and contain (except the 3×10^{17} cm^{-2} sample) narrow TE and TM modes clearly re-

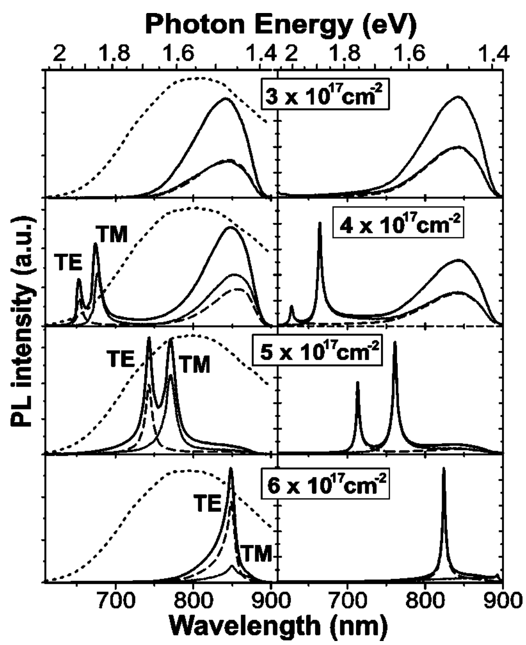

FIG. 2. Left column: Experimental PL spectra for layers implanted with doses 3, 4, 5, and 6×10^{17} Si cm^{-2} (from top down) detected in two different directions: The conventional normal incidence PL spectra (broad dotted line) and PL spectra emanating from the facet of the sample [black line—PL without polarizer, dashed line—with polarizer parallel to the layer (TE mode), short-dashed lines—polarizer perpendicular to the layer (TM mode)]. Right column: Calculated PL spectra from the sample facet ($\alpha = 0°$), taking into account the detection NA=0.075. The broad emission bands appearing in the samples 3×10^{17} Si cm^{-2} and 4×10^{17} Si cm^{-2} represent guided modes scattered into the detector collection angle.

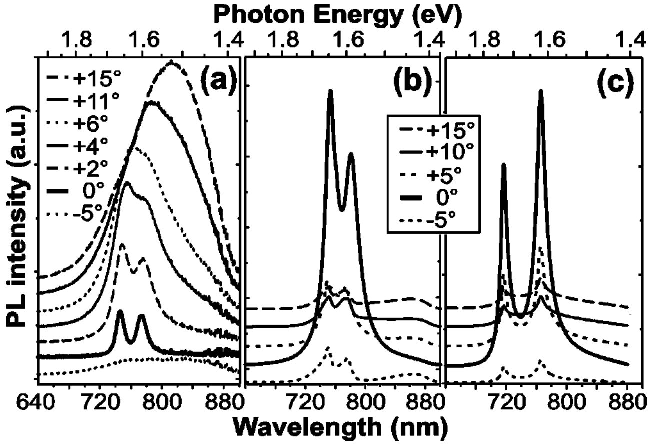

FIG. 3. Angular dependencies (sample 5×10^{17} Si cm^{-2}): Unpolarized PL spectra measured at various angles α with respect to the normal to the output facet in the sample 5×10^{17} Si cm^{-2} using either the goniometer setup (a) or the micro-PL setup (b). The angular resolution is about 8.6° and 1°, respectively. Panel (c) represents model calculations of the angular dependence for aperture collection angle of 8.6°.

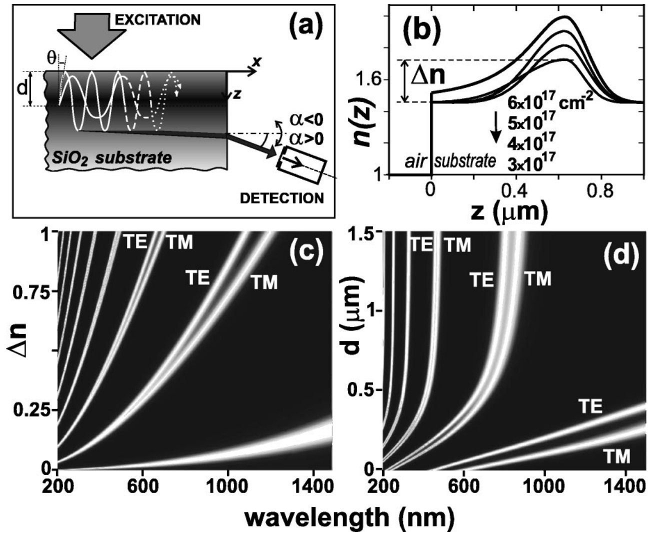

FIG. 4. (a) Cross section of the Si-NC planar waveguide with a graded index profile $n(z)$. Rays of both guided and substrate modes are indicated. (b) Refractive index profiles $n(z)$ in the investigated samples. Lower two panels show calculated spectral positions of the substrate modes: As a function of the refractive index contrast Δn (c) and as a function of the maximum index contrast depth d in the sample 5×10^{17} Si cm^{-2} (d).

solved with a linear polarization filter parallel (TE) or perpendicular (TM) to the layer edge. Such surprising PL spectra from a simple layer of Si-NCs have been reported for the first time only recently.[13,14] Typical PL spectra from Si-NCs consist of a broad band centered at 700–800 nm with FWHM of 150–200 nm, consistent with the dotted curves in Fig. 2.

We stress that the TE/TM mode structure is only resolved in PL spectra collected in a direction close to $\alpha=0°$ (i.e., detection axis lying in the implanted plane). This is clearly illustrated in Fig. 3(a) where PL spectra for several collection angles α are plotted. These results were obtained using the goniometer setup [Fig. 1(b)] with an angular resolution of about 1°. In this case, however, all emission propagating towards the collecting optical fibre is detected. Only in the micro-PL setup we can separate the contribution of light guided along the implanted layer from normal incidence light emission [Fig. 1(a)]. The angular dependence of the separated edge emission is shown in Fig. 3(b) where one can see clear mode structure emitted preferentially to the $\alpha=0°$ direction.

The crucial question to be addressed is how do these narrow lines originate? The waveguide formed by the Si-NC plane "buried" in the SiO_2 matrix is shown schematically in Fig. 4(a). The refractive index profile $n(z)$ across the layer is determined by the Si-NC distribution beneath the surface. Such profiles were obtained by fitting interference fringes in visible-infrared transmission spectra of Si-NC layers (not shown here). These $n(z)$ profiles are displayed in Fig. 4(b) for each of the samples investigated. Their differences from the substrate refracted index $n_{\text{sub}}=1.455$ are approximated either by nonsymmetric Gaussian or by Gaussian-Lorentzian curves. The depth of the maximum refractive index contrast Δn below the surface was found to be $d=0.63$ μm in all samples and the profiles are asymmetric, tailing towards the surface, consistent with the implanted Si distribution (not shown).

Figure 4(a) summarizes the following reasoning in the framework of a ray scheme. PL rays, emerging (at depth d) at high enough angles θ, undergo total internal reflection at the core-cladding interface and propagate within the Si-NC core region as normal guided modes (representing continuous spectrum). However, rays emerging at angles θ that are close but slightly below the critical angle $\theta_c=\arcsin[n_{\text{sub}}/(n_{\text{sub}}+\Delta n)]$ for total reflection at the core-substrate interface can reach the sample surface $z=0$ and be totally reflected at this boundary.[15] This reflection introduces an extra steplike phase shift that causes the splitting of the TE and TM modes.[16,17] The reflected beam then propagates through the core region and undergoes partial reflection from the core-substrate interface. At each such reflection a small part of energy of modes can leak out from the Si-NC layer into the SiO_2 matrix as a substrate mode[18] that finally leaves the sample facet at the detection angle α close to zero [Fig. 4(a)].

It is now demonstrated that this model can simulate the experimental emission spectra with high fidelity when taking into consideration these substrate modes. We assume isotropic radiation of randomly oriented dipoles (Si-NC) that are randomly scattered inside the waveguide (i.e., we neglect their positions with respect to the z axis which would become important when studying microcavity effects). The interest here is on the mode energy, i.e., the output PL intensity, as a function of the angle θ and wavelength λ.[19] With the aid of equations for deriving the cavity enhancement factor[20] we get for the mode amplitude inside the waveguide

$$A(\theta,\lambda)=A_0/(1-tr_1r_2),$$

where A_0 is an effective source strength and $t<1$ is a transmission coefficient [in general $t=t(\theta,\lambda)$] during one roundtrip of the wave in the waveguide. r_1 and r_2 are the reflectivities of the waveguide boundaries that can be calculated (see, e.g., 16) by using a transfer-matrix method. The transfer matrix M is calculated as $M=M_1M_2M_3\cdots M_n$, where

M_k, $0<k\leq n$, are transfer matrices for very thin layers into which the structure was "cut," in parallel with the sample surface, for the purpose of numerical calculation. The intensity of a mode is proportional to AA^*. In the present study we used $t=0.995$ [in agreement with experimentally established damping of about 10 cm^{-1} (Ref. 21)] and $n=5000$.

The results of calculations are presented in Fig. 2 (right column). The overall agreement with the experimental data (left column) is excellent, providing strong support for the proposed model that the observed PL spectral narrowing and TE/TM splitting are due to the substrate modes propagating nearly in parallel with the boundary of the waveguide. (We should note that the intensity of the calculated modes here has been modulated by the spontaneous broad PL emission band to allow direct comparison with experiment.) One can easily recognize in Fig. 2 a TE/TM "doublet" whose spectral position is red shifting and the separation between components is increasing with increasing implantation dose. This behavior is displayed more generally in Fig. 4(c) (calculated mode position as a function of the maximum index contrast Δn, which is linked to the implantation energy) and Fig. 4(d) (calculated mode position as a function of the depth d). Similar calculations were performed for the angular dependence of PL for the layer 5×10^{17} Si cm^{-2} and the results are displayed in Fig. 3(c). One can clearly see the narrow modes at angles close to $\alpha=0$ in good agreement with the experimental results [Fig. 3(b)].

The question that remains is why the substrate modes are so significant here. A likely answer to this question is that the regular guided modes experience greater loss during their propagation in the plane of the waveguide. Indeed, the beams responsible for generating the substrate modes travel reduced distances through the core region and once launched, the substrate mode undergoes virtually no loss in traveling to the substrate facet. On the other hand, the standard guided modes are strongly damped on their trip over a macroscopic distance from the place of creation towards the sample edge due to absorption and scattering. The model employed here does not depend on the nature of the core losses but simply on the fact that the loss is significant. The most likely source of loss in the present case is absorption and scattering from nanocrystals, as well as scattering from the "interface" between the core and cladding layers. The latter likely arises from the implantation process where the penetration depth of the Si^+ ions directly reflects the surface roughness of the polished silica substrate, which is of the order of ±10 nm. It is known that microphotonic etched waveguide structures suffer from optical scattering loss due to sidewall roughness and that this loss increases with increasing refractive index contrast Δn.[22] The contribution of this later process is supported by the fact that these substrate modes do not reveal themselves in the edge emission of waveguides with atomically flat sidewalls.

IV. CONCLUSIONS

It has been demonstrated, both experimentally and theoretically, that continuous wave PL can propagate in specific narrow band, highly directional, substrate modes instead of normal guided modes in an active planar optical waveguide. We have analyzed a waveguide made of Si-NCs but the effect is a general property of asymmetric thin films. The waveguide self-selects these modes from the broadband PL emission of the core. The spectral distribution and experimental manifestation of such modes is critically dependent upon several waveguide parameters, predominantly the refractive index difference between the core and cladding/substrate (determined by the implantation dose in the present study), the waveguide loss, the depth d of Si-NCs distribution beneath the surface and also upon the shape of $n(z)$. The role of these modes in facilitating/hampering optical gain requires further analysis.[11]

ACKNOWLEDGMENTS

This work was sponsored by Grant No. 202/03/0789 of GACR, Project No. IAA1010316 of GAAVCR, Ministry of Education of CR project ME 486, Royal Swedish Academy of Sciences and by the Australian Research Council. The authors thank F. Trojanek for help with calculations and A. Poruba, A. Fejfar, and K. Kusova for experimental assistance.

[1] L. T. Canham, Appl. Phys. Lett. **57**, 1046 (1990).
[2] L. Pavesi, L. Dal Negro, C. Mazzoleni, G. Franzo, and F. Priolo, Nature (London) **408**, 440 (2000).
[3] L. Khriachtchev, M. Räsänen, S. Novikov, and J. Sinkkonen, Appl. Phys. Lett. **79**, 1249 (2001).
[4] M. H. Nayfeh, N. Barry, J. Therrien, O. Akcakir, E. Gratton, and G. Belomoin, Appl. Phys. Lett. **78**, 1131 (2001).
[5] M. Ivanda, U. V. Desnica, C. W. White, and W. Kiefer, in *Towards the First Silicon Laser*, NATO Science Series II. Mathematics, Physics and Chemistry, Vol. 93, edited by L. Pavesi, S. Gaponenko, and L. Dal Negro (Kluwer Academic, Dordrecht, 2003), p. 191.
[6] P. M. Fauchet and J. Ruan, in *Towards the First Silicon Laser*, NATO Science Series II. Mathematics, Physics and Chemistry, Vol. 93, edited by L. Pavesi, S. Gaponenko, and L. Dal Negro (Kluwer Academic, Dordrecht, 2003), p. 197.
[7] L. Dal Negro, M. Cazzanelli, L. Pavesi, S. Ossicini, D. Pacifici, G. Franzo, F. Priolo, and F. Iacona, Appl. Phys. Lett. **82**, 4636 (2003).
[8] C. Y. Hu, H. Z. Zheng, J. D. Zhang, H. Zhang, F. H. Yang, and Y. P. Zeng, Appl. Phys. Lett. **82**, 665 (2003).
[9] J. L. Shen, J. Y. Chang, H. C. Liu, W. C. Chou, Y. F. Chen, T. Jung, and M. C. Wu, Solid State Commun. **116**, 431 (2000).
[10] D. T. Shaafsma and D. H. Christensen, Phys. Rev. B **54**, 14618 (1996).
[11] A. Penzkofer, W. Holzer, H. Tillmann, and H.-H. Hőrhold, Opt. Commun. **229**, 279 (2004).
[12] V. Kiisk, I. Sildos, A. Suisalu, and J. Aarik, Thin Solid Films **400**, 130 (2001).
[13] J. Valenta, I. Pelant, K. Luterová, R. Tomasiunas, S. Cheylan, R. G. Elliman, J. Linnros, and B. Hőnerlage, Appl. Phys. Lett. **82**, 955 (2003).
[14] L. Khriachtchev, M. Räsänen, S. Novikov, Appl. Phys. Lett. **83**, 3080 (2003).
[15] The angle of incidence on the (sample/air) boundary is, due to the graded index profile, greater than the critical angle $\theta_c'=\arcsin[1/(n(z=0))]$ for all index profiles displayed in Fig. 4(b).
[16] P. Yeh, *Optical Waves in Layered Media* (Wiley, New York, 1988).
[17] M. Born and E. Wolf, *Principles of Optics* (Pergamon, Oxford, 1968).
[18] We stress that this is not an *evanescent* wave connected with the guided modes. Such waves cannot contribute to the far-field radiation. See E. Wolf and J. T. Foley, Opt. Lett. **23**, 16 (1998).
[19] Note that the detection angle α is linked to the angle θ through $\sin\alpha = n_{\mathrm{substrate}}\sin\{\pi/2-\arcsin[(n_{\mathrm{substrate}}+\Delta n)\sin\theta/n_{\mathrm{substrate}}]\}$.
[20] R. Baets, P. Bienstman, and R. Bockstaele, in *Confined Photon Systems*, edited by H. Benisty, J.-M. Gérard, R. Houdré, J. Rarity, and C. Weisbuch (Springer, Berlin, 1999), Vol. 531.
[21] J. Valenta, I. Pelant, and J. Linnros, Appl. Phys. Lett. **81**, 1396 (2002).
[22] J. H. Jang *et al.*, Appl. Phys. Lett. **83**, 4116 (2003).